ARTICLE OPEN

Check for updates

Atrophy in preclinical Alzheimer's disease maps to a network that predicts longitudinal decline

Soyoung Lee[1,2✉], Sheena R. Baratono[1,3], Junghee Ha[1,2], Grace T. Burt[1,3], Stephan T. Palm[1,4], William J. Drew[1,3], Benjamin S. Zide[2], Nicole M. Chiulli[1,4], Sara Lariviere[5], Shaoshi Zhang[1,4,6], B. T. Thomas Yeo[6], Michael D. Fox[1,3], Reisa A. Sperling[3,7], Nancy J. Donovan[2,3,8] and Shan H. Siddiqi[1,4]

Brain atrophy may precede cognitive and functional impairment in Alzheimer's disease (AD), but at this "preclinical" stage, it remains unclear whether atrophy localizes to specific brain networks and whether such localization is associated with clinical outcomes. We investigated cortical thickness in 1778 cognitively unimpaired (CU) older adults with amyloid-β (Aβ) PET from the A4 (Anti-Amyloid Treatment in Asymptomatic Alzheimer's Disease) and LEARN (Longitudinal Evaluation of Amyloid Risk and Neurodegeneration) studies, with a subset ($N = 445$) with tau PET. We estimated the networks disrupted by each individual's cortical thinning using a large normative connectome database ($N = 1000$), and tested whether this preclinical AD atrophy network is associated with clinical manifestations and longitudinal cognitive (PACC) and functional (CDR) trajectories. Distinct networks connected to atrophy patterns were associated with Aβ and regional tau in CU older adults. These networks were similar to a previously published atrophy network for AD dementia (Aβ: $r = 0.817$, $P = 0.006$; tau: $r = 0.712$, $P = 0.046$). Atrophy connectivity to this preclinical AD network was associated with higher Aβ and tau, independent of total cortical atrophy, and cross-sectionally with lower cognition, greater subjective cognitive decline, and increased anxiety; longitudinally, it predicted faster cognitive and functional decline over ~5 years. After tau adjustment, the functional-decline effect was preserved while the cognitive-slope effect was largely attenuated. Atrophy in preclinical AD localizes to a network resembling AD dementia, and is independently associated with AD pathologies, clinical outcomes, and longitudinal decline. Network-level neurodegeneration is detectable and clinically informative in preclinical AD, supporting future network-based research and therapeutic development.

Molecular Psychiatry; https://doi.org/10.1038/s41380-026-03706-0

INTRODUCTION

Alzheimer's disease (AD) pathologic changes, including abnormal accumulation of amyloid-β (Aβ) and tau, begin many years before individuals develop cognitive and functional impairment [1]. It remains unclear whether Aβ and tau accumulation are associated with a distinct pattern of network-level atrophy during this "preclinical" stage, when individuals remain cognitively unimpaired (CU). Defining atrophy-related brain networks and clinical manifestations in preclinical AD is critical to understanding initial AD pathophysiology and could lead to better prediction of disease trajectories and to novel diagnostic and treatment strategies.

Studies of atrophy in preclinical AD have yielded mixed results. At this stage, distinguishing AD-associated atrophy from age-related volume loss or early atrophy from other neurodegenerative conditions is difficult, as atrophy emerges later than Aβ and tau pathologies [2]. Some studies support that AD-specific cortical thinning occurs in preclinical AD [3, 4], while others have found no cross-sectional difference [5] or even increased cortical thickness [6]. Methodological and technical differences across studies, heterogeneity in the preclinical phase, and inadequate sample size may contribute to these discrepancies [7, 8].

Mapping lesion-induced symptoms onto the functional brain networks rather than individual brain locations has allowed the localization of various neurologic and psychiatric symptoms [9]. Recent work suggests that this lesion network mapping technique may be applied to neurodegenerative conditions, using atrophy as the "lesion." Tetreault et al. demonstrated that atrophy locations in individual patients map to brain networks associated with clinical, cognitive, and neuropsychiatric symptoms of AD dementia [10]. However, this atrophy network mapping (ANM) has never been implemented in preclinical AD, and it is unclear whether the method can detect subtle changes in cortical thickness at this stage.

Here, we use ANM [Fig. 1] to investigate network-level neurodegeneration and its association with pathological and clinical manifestations in CU older adults using a large, well-

[1]Center for Brain Circuit Therapeutics, Brigham and Women's Hospital, Boston, MA, USA. [2]Division of Geriatric Psychiatry, Department of Psychiatry, Brigham and Women's Hospital, Harvard Medical School, Boston, MA, USA. [3]Department of Neurology, Brigham and Women's Hospital, Harvard Medical School, Boston, MA, USA. [4]Department of Psychiatry, Brigham and Women's Hospital, Harvard Medical School, Boston, MA, USA. [5]Department of Nuclear Medicine and Radiobiology, Université de Sherbrooke, Sherbrooke, QC, Canada. [6]Centre for Sleep and Cognition & Centre for Translational Magnetic Resonance Research, Yong Loo Lin School of Medicine, National University of Singapore, Singapore, Singapore. [7]Department of Neurology, Massachusetts General Hospital, Harvard Medical School, Boston, MA, USA. [8]Department of Psychiatry, Massachusetts General Hospital, Harvard Medical School, Boston, MA, USA. ✉email: Soyoung.Lee@bwh.harvard.edu

Received: 3 May 2026 Revised: 12 May 2026 Accepted: 16 June 2026
Published online: 26 June 2026

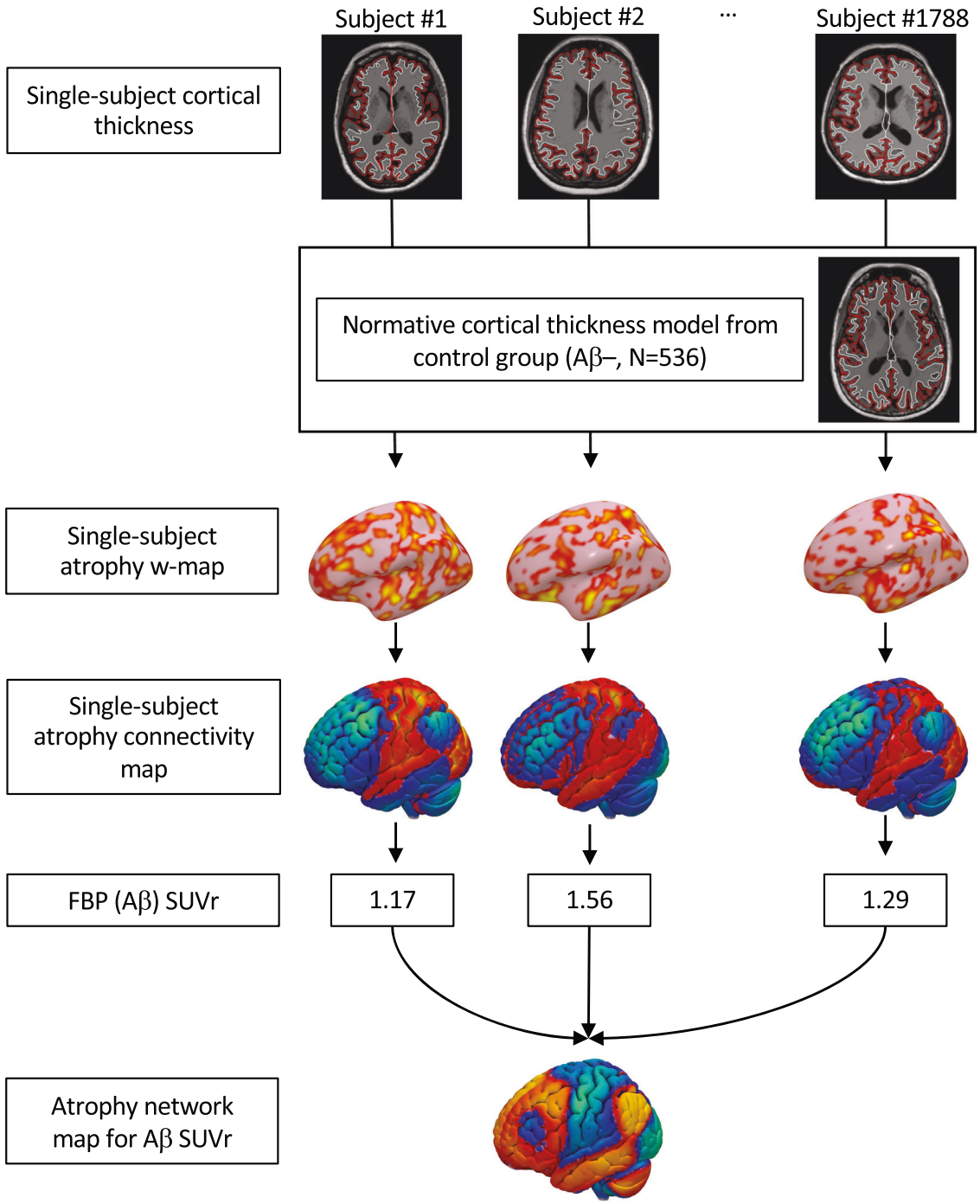

Fig. 1 Atrophy Network Mapping (ANM). ANM was performed in the A4/LEARN dataset ($N = 1778$) following Tetreault et al. [10]. Briefly, vertex-wise atrophy w-scores (z-scores adjusted for age and sex relative to the Aβ−CU normative sample) were computed for each participant and projected through a normative functional connectome (Brain Genomics Superstruct Project, $N = 1000$) [32, 33] to derive participant-specific atrophy connectivity maps. To identify network patterns associated with AD pathology, voxel-wise ANCOVA (adjusted for age and sex) compared atrophy connectivity maps between Aβ+ and Aβ− groups, with FWE correction [31]. The analysis was repeated with continuous Aβ SUVr to maximize statistical power, and additionally adjusting for covariates.

characterized cohort from an AD prevention clinical trial in preclinical AD [11, 12], and validate ANM by comparing it to a previously published atrophy network for AD dementia derived from a longitudinal, multi-center, observational study of AD [13]. We hypothesized that (1) atrophy in the preclinical stage of AD would localize to a distinct brain network, (2) this preclinical AD network would be similar to atrophy patterns previously implicated in AD dementia, and (3) this preclinical AD network would be associated with cognition, neuropsychiatric symptoms, and longitudinal cognitive and functional decline.

METHODS AND MATERIALS

Participants

Cross-sectional and longitudinal data from cognitively unimpaired (CU) older adults were obtained from the Anti-Amyloid Treatment in

Asymptomatic Alzheimer's Disease (A4, NCT02008357) and Longitudinal Evaluation of Amyloid Risk and Neurodegeneration (LEARN, NCT02488720) dataset (https://ida.loni.usc.edu/login.jsp). The A4 study was a double-blind, placebo-controlled, secondary-prevention trial of solanezumab in CU older adults with elevated brain Amyloid-β (Aβ+); LEARN was an observational companion study of CU older without elevated brain Aβ (Aβ). Screening procedures are described previously [12]. Data from the Alzheimer's Disease Neuroimaging Initiative (ADNI) [13] (adni.loni.usc.edu) were used to replicate the AD-dementia atrophy network published by Tetreault et al. All studies were IRB-approved, and written consents were obtained from all participants.

Demographics, genetic information, and clinical assessments

The A4/LEARN data included demographic information, including age, *sex*, and *years of education*, dichotomized *Apolipoprotein E ε4 (APOE4) carrier status, and treatment group (placebo vs. solanezuma; A4* (Aβ+) group only). ***Cognitive performance*** was assessed by the *Preclinical Alzheimer Cognitive Composite (PACC)* [14, 15], and its subdomains, the *Logical Memory Delayed Recall (Logical Memory)*, the Mini-Mental Status Exam (*MMSE*), the *Weschler Adult Intelligence Scale-Revised Digit Symbol Coding (Digit Symbol)*, and the *Free and Cued Selective Reminding Test (FCSRT)*. ***Subjective cognitive decline*** was assessed using the *Cognitive Function Index (CFI)*, administered individually to the participant (CFI-PT) and their study partner (CFI-SP) [16, 17]. ***Global cognitive/functional status*** was assessed by the *Clinical Dementia Rating (CDR)* [18]. ***CDR-Global progression event*** is defined as previously described [11]. Neuropsychiatric and behavioral variables included ***Anxiety*** (*State-Trait Anxiety Inventory [STAI-6])* [19], ***depression*** (*Geriatric Depression Scale [GDS])* [20], and ***perception of one's future*** (*Future Time Perspective Scale [FTPS])* [21], and lifetime histories of suicidal attempts and passive death wishes. Detailed descriptions of the assessments and ADNI variables are reported in the Supplement.

Neuroimaging acquisition and processing

3T structural MRI T1 images were processed using Freesurfer 6.0 [22]. *Global cortical thickness* was computed by averaging across all cortical vertices, and the *hippocampal occupancy* score, the ratio of hippocampal volume to the sum of the hippocampal and inferior lateral ventricle volumes, was used as provided [23].

All participants underwent Aβ PET using ^{18}F-florbetapir (FBP) [12]. Aβ status (Aβ+ vs. Aβ–) was determined using a dual quantitative and qualitative method (whole-cerebellum-normalized SUVr ≥ 1.15, with intermediate values 1.10–1.15 confirmed by visual read) [24]. A subset of participants underwent ^{18}F-flortaucipir (FTP) [25] tau PET with partial-volume-corrected SUVr from the PetSurfer pipeline [26, 27]. ADNI subjects' Aβ status was determined using the same FBP cut-off .

Statistical analyses

Computational neuroimaging analyses used MATLAB R2022b; [28] statistical analyses used R 4.3.1 [29].

Cross-sectional cortical thickness comparisons. Global cortical thickness, hippocampal occupancy, and vertex-wise cortical thickness were compared between Aβ+ and Aβ− groups using t-tests and ANCOVA (covariates: age, sex, years of education, *APOE* ε4 status). Vertex-wise analyses were also performed using continuous Aβ SUVr [30]. Vertex-wise comparisons were corrected by family-wise error (FWE; permutation-based max-t) [31].

Atrophy Network Mapping (ANM). [Figure 1] ANM was performed in the A4/LEARN dataset ($N = 1778$) following Tetreault et al. [10]. Briefly, vertex-wise atrophy w-scores (z-scores adjusted for age and sex relative to the Aβ −CU normative sample) were computed for each participant and projected through a normative functional connectome (Brain Genomics Superstruct Project, $N = 1000$) [32, 33] to derive participant-specific atrophy connectivity maps. To identify network patterns associated with AD pathology, voxel-wise ANCOVA (adjusted for age and sex) compared atrophy connectivity maps between Aβ+ and Aβ− groups, with FWE correction [31]. The analysis was repeated with continuous Aβ SUVr to maximize statistical power, and additionally with education and *APOE* status as covariates. The same procedure was applied to ADNI-2 ($N = 233$) [13] to replicate the AD-dementia atrophy network. Spatial similarity between maps was tested by permutation (1000 iterations) [34]. Tau-based ANM was performed in the tau subset ($N = 445$) using inferior-temporal SUVr and a meta-temporal composite (entorhinal, amygdala, parahippocampal, fusiform, inferior temporal, middle temporal; corresponding to Braak stages I–V) [35–37]. Full ANM procedural details are in the Supplement.

Cross-sectional associations: Leave-one-out and 20-fold cross-validation *frameworks*. To evaluate associations between an individual's atrophy in the preclinical AD network and AD-related neuroimaging or clinical features, we used two complementary cross-validation approaches. First, leave-one-out (LOO) preclinical AD networks were generated by re-running the Aβ-based ANM on all participants except a held-out subject; that subject's **'network atrophy'** was defined as *the spatial correlation between their atrophy connectivity map and the LOO preclinical AD network*. Second, to further validate the associations, a 20-fold cross-validation was performed, repeated 10 times with unique random splits, yielding 200 fold-level statistics per feature. Significance for the 20-fold framework was determined using [38] Nadeau and Bengio's corrected resampled t-test to account for repeated-CV data overlap, with Benjamini–Hochberg FDR correction [39] Compared variables included Aβ status, continuous Aβ SUVr, regional tau SUVr, global cortical thickness, PACC and subdomains, CFI (PT and SP), STAI-6 and worry items, GDS, FTPS, and lifetime suicide attempts/death wishes. Full procedural details for both LOO and 20-fold methods are in the Supplement.

Longitudinal analyses. Longitudinal cognitive decline (PACC) was modeled with linear mixed-effects (LME) models (REML; *nlme*) with random intercepts and random slopes for time (weeks since baseline). The primary model tested whether baseline network atrophy moderated the rate of cognitive decline (Weeks × network atrophy interaction), adjusting for age, sex, years of education, *APOE* ε4, mean cortical thickness, Aβ SUVr, and treatment (in A4 only). Predicted PACC change from baseline was visualized at the sample mean ± 1 SD of network atrophy. To quantify the unique contribution of network atrophy beyond established AD risk factors, semi-partial marginal R^2 [40] was computed for each predictor.

Functional decline was modeled using Cox proportional-hazards regression with global CDR progression as the outcome and time in weeks; follow-up was administratively censored at week 240. Network atrophy was z-standardized so the hazard ratio reflects per-1-SD change. Covariate-adjusted survival curves were generated at low (−1 SD), mean, and high (+1 SD) baseline network atrophy. The proportional-hazards assumption was verified with scaled Schoenfeld residuals. All longitudinal analyses were performed in the full cohort and stratified by Aβ status. Sensitivity analyses adjusted for baseline regional tau (inferior-temporal SUVr; meta-temporal composite). Detailed model specifications and full coefficient tables are in Supplementary Methods and Tables S2–S11.

RESULTS

Sample characteristics

The A4/LEARN sample comprised 1778 CU older adults (Aβ−: $N = 536$; Aβ+: $N = 1242$). Mean (SD) age was 71.5 (4.7) years; 1060 (59.6%) were female; mean education was 16.6 (2.8) years. Aβ+ participants were older ($P < 0.001$), had lower PACC ($P < 0.001$), and reported greater CFI ($P < 0.001$) than Aβ− participants, adjusting for demographics, consistent with prior reports [12] [Table 1].

Conventional cortical-thickness measures did not differ by Aβ status

Global cortical thickness and hippocampal occupancy did not differ significantly between Aβ+ and Aβ− groups [Table 1], adjusting for demographics. The cortical thickness in both Aβ+ and Aβ– groups was highly heterogeneous; the average cortical thickness within each group is depicted in Supplementary Fig. 1A and B. Vertex-wise comparison showed no regions surviving FWE correction. [Supplementary Fig. 1C] Continuous Aβ SUVr correlated with scattered small clusters of cortical thinning in the superior frontal gyrus, postcentral gyrus, posterior cingulate/precuneus, superior temporal gyrus, parahippocampal gyrus, and cuneus ($P_{FWE} < 0.05$). [Supplementary Fig. 1D].

Table 1. Baseline characteristics of A4/LEARN cohort by amyloid-β status.

Variable	Total ($N = 1778$)[a]	Aβ− ($N = 536$)[a]	Aβ+ ($N = 1242$)[a]	p
Age (years)	71.54 (4.74)	70.46 (4.29)	72.00 (4.84)	<0.001
Female, n (%)	1060 (60%)	328 (61%)	732 (59%)	0.373
Education (years)	16.62 (2.76)	16.76 (2.62)	16.56 (2.81)	0.149
APOE ε4 carrier, n (%)	849 (48%)	127 (24%)	722 (58%)	<0.001
PACC	−0.20 (2.63)	0.28 (2.41)	−0.41 (2.69)	0.003
Digit Symbol	43.06 (8.93)	44.15 (8.82)	42.59 (8.93)	0.198
FCSRT	75.88 (6.04)	76.72 (5.71)	75.52 (6.14)	0.018
Logical Memory (delayed)	11.56 (3.34)	11.89 (3.35)	11.42 (3.32)	0.100
MMSE	28.80 (1.24)	28.94 (1.13)	28.75 (1.28)	0.054
CFI total	7.35 (6.25)	6.02 (5.65)	7.93 (6.41)	<0.001
CFI – Study Partner	3.04 (3.81)	2.44 (3.26)	3.30 (4.00)	<0.001
CFI – Participant	4.31 (3.83)	3.58 (3.55)	4.63 (3.91)	<0.001
Mean cortical thickness (mm)	2.18 (0.08)	2.19 (0.08)	2.18 (0.08)	0.230
Hippocampal occupancy	0.73 (0.08)	0.76 (0.07)	0.73 (0.08)	0.508
Aβ PET SUVr	1.23 (0.22)	0.99 (0.07)	1.33 (0.18)	<0.001

Continuous variables are presented as mean (standard deviation); Female and APOE ε4 carrier are presented as n (%). For demographic and genetic variables (age, sex, education, APOE ε4 carrier status), *p*-values are from independent-samples t-tests (continuous) or the chi-square test (binary), unadjusted. For cognitive and neuroimaging measures, *p*-values are adjusted for age, sex, and years of education using linear regression.
PACC preclinical alzheimer cognitive composite, *Digit Symbol* digit symbol substitution test (wechsler adult intelligence scale–revised), *Logical Memory (delayed)* logical memory iia subtest (wechsler memory scale), *FCSRT* free and cued selective reminding test, *MMSE* mini-mental state examination, *CFI* cognitive function index, *SP* study partner, *PT* participant, *SUVr* standardized uptake value ratio. Hippocampal occupancy was computed as the ratio of hippocampal volume to the sum of hippocampal and inferior lateral ventricle volumes in each hemisphere, averaged across hemispheres, and normalized for age and sex.
[a]Mean (SD); n (%).

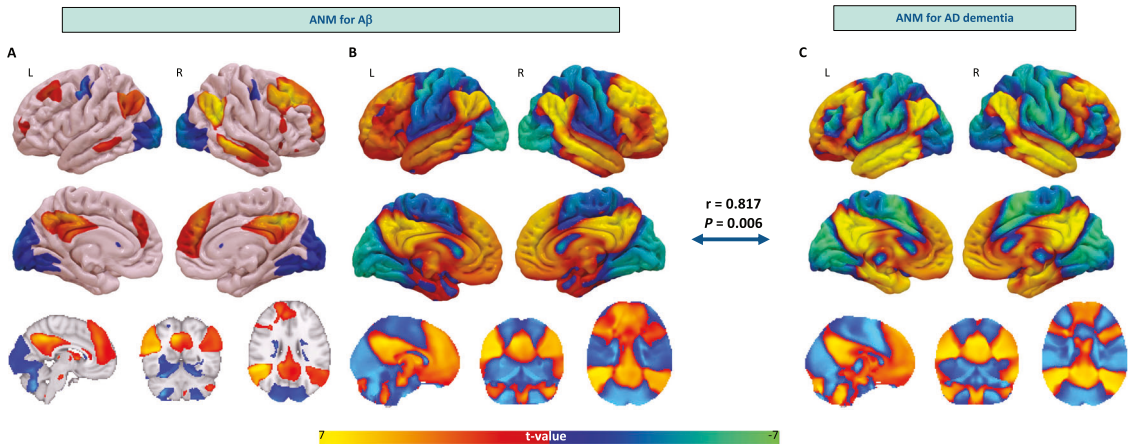

Fig. 2 Localizing network-level atrophy in preclinical Alzheimer's disease (AD) using Atrophy Network Mapping (ANM) for amyloid-β (Aβ). A Atrophy network map for preclinical Alzheimer's disease using continuous **Aβ**: voxel-wise linear regression of functional connectivity to atrophy and Aβ SUVr using Pearson correlation, adjusting for age and sex. Family-wise-error (FWE)-corrected ($P < 0.05$). **B** Atrophy network map for preclinical AD (Aβ), uncorrected. **C** A replication of a previously published atrophy network map for Alzheimer's disease dementia by Tetreault et al. from the Alzheimer's Disease Neuroimaging Initiative (ADNI) II dataset, uncorrected. **Comparison between the atrophy network map for preclinical AD vs. the atrophy network map for AD dementia:** The preclinical AD map (**B**) was compared to AD dementia map (**C**) derived from the ADNI-2 dataset. The spatial correlation coefficient between these two maps was 0.817, and the *P*-value from a random permutation test (number of iterations = 1000) was 0.006.

Atrophy network map for preclinical AD

ANM in the A4/LEARN sample ($N = 1778$) [Fig. 2] identified atrophy patterns connected to a distinct network associated with Aβ pathology. Using continuous Aβ SUVr increased sensitivity over dichotomous Aβ+/− comparisons [Supplementary Fig. 1E]; the resulting "preclinical AD network" included dorsolateral and medial prefrontal lobes, precuneus, lateral parietal lobe, temporoparietal junction, and middle temporal gyrus ($P_{FWE} < 0.05$) [Fig. 2A]. Subsequent analyses used continuous-Aβ ANM as the primary preclinical AD network.

The preclinical AD network was highly similar to the AD-dementia atrophy network derived from ADNI-2 (spatial $r = 0.817$, $P = 0.006$; Fig. 2B, C), indicating that atrophy connectivity in preclinical AD localizes to a network resembling that of overt AD dementia.

Tau-based atrophy networks resembled the Aβ-based preclinical AD network

In the tau-PET subset ($N = 445$), atrophy patterns associated with greater inferior-temporal tau SUVr were connected to a network most similar to the Aβ-based preclinical AD network ($r = 0.86$,

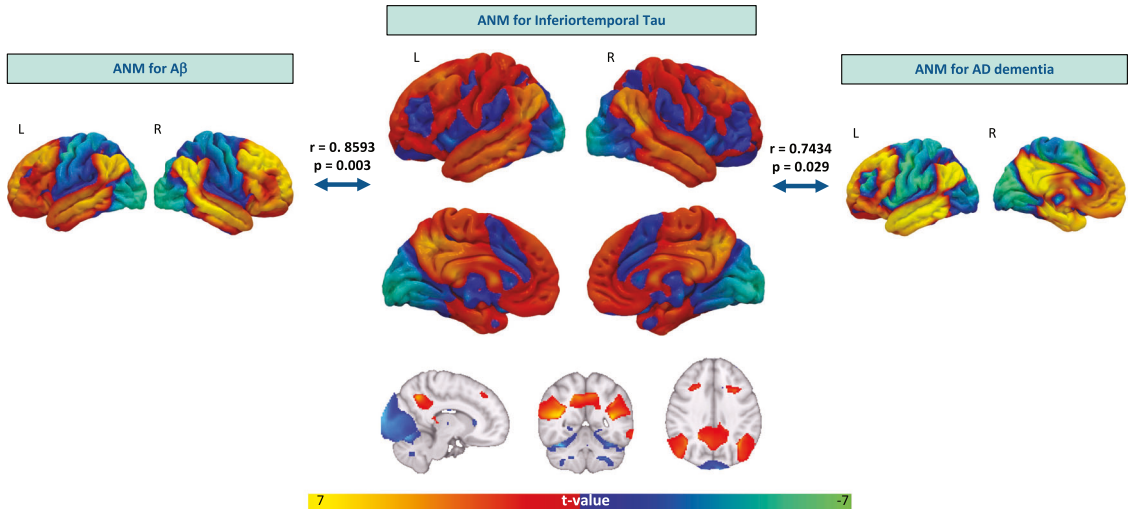

Fig. 3 Localizing network-level atrophy in preclinical Alzheimer's disease (AD) using Atrophy Network Mapping (ANM) for the inferiortemporal tau. Voxel-wise linear regression of functional connectivity to atrophy and **tau** SUVr in the bilateral inferiortemporal cortices using Pearson correlation, adjusting for age and sex. This map was similar to **the atrophy network map for preclinical AD based on amyloid-β (Aβ)** (spatial r = 0.7878, $P = 0.014$ by random permutation testing) and to **the atrophy network map for AD dementia from the ADNI-2 dataset** (spatial r = 0.7115, $P = 0.046$). Below is the ANM of preclinical AD based on tau, Family-wise-error (FWE)-corrected ($P < 0.05$).

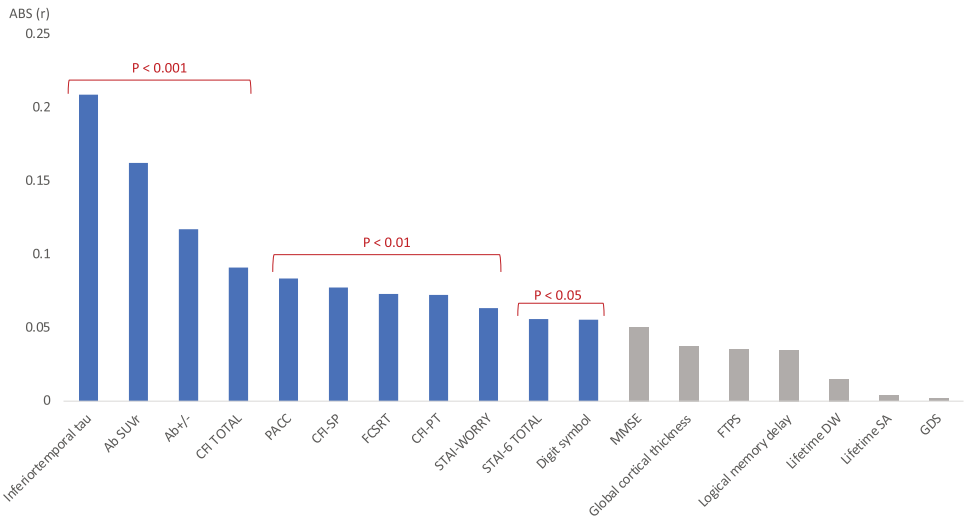

Fig. 4 20-Fold Cross-validation: Cross-sectional association of Atrophy Connectivity to Preclinical AD Network with Alzheimer's pathology and clinical variables. "Network Atrophy," spatial correlation between the given participant's atrophy connectivity map and the preclinical Alzheimer's disease network identified by Atrophy Network Mapping, was associated with Inferiortemporal (IT) tau SUVr*, Amyloid-β (Aβ) SUVr, dichotomous Aβ+/− group, global average cortical thickness, cognition (PACC), subjective cognitive decline (CFI), anxiety (STAI-6), and worry symptom (STAI-worry) but not with depression (GDS). Some of the PACC subdomains and other non-AD-specific behavioral variables, such as FTPS, Lifetime DW, and Lifetime SA, were significantly associated with network atrophy. * Association with IT tau was tested in the subgroup with tau PET ($N = 445$). PACC preclinical alzheimer cognitive composite, Digit Symbol digit symbol substitution test score from the wechsler adult intelligence scale-revised, Logical Memory Delay logical memory IIa sub-test from the wechsler memory scale, FCSRT free and cued selective reminding test, MMSE mini-mental status exam, CFI cognitive function inventory, SP study partner, PT participant. FTPS future time perspective scale, GDS geriatric depression scale, DW death wish, SA suicidal attempt.

$P = 0.003$) and to the AD-dementia network (r = 0.74, $P = 0.029$) [Fig. 3]. Peak locations included precuneus, lateral parietal lobe, prefrontal lobe, temporoparietal junction, and middle temporal gyrus. Tau-based maps using other meta-temporal ROIs [37] showed similar patterns (spatial r vs. Aβ-based map: 0.59–0.82; Supplementary Fig. 2).

Network atrophy was associated with Aβ, tau, cognition, and anxiety cross-sectionally

In 1778 participants, each individual's 'network atrophy,' *the spatial correlation between their atrophy connectivity map and the preclinical AD network*, was computed using leave-one-out (LOO) cross-validation (CV), and cross-sectional associations were further validated by 20-fold CV. Network atrophy was associated with Aβ status (r = 0.12, $P = 2.5 \times 10^{-6}$) and continuous Aβ SUVr (r = 0.16, $P = 8.2 \times 10^{-10}$) [Fig. 4]. The Aβ-SUVr association was independent of global cortical atrophy (partial r = 0.16, $P = 1.5 \times 10^{-10}$), and network atrophy was not associated with global cortical thickness (r = 0.04, $P = 0.12$). In the tau subset ($N = 445$), network atrophy correlated with inferior-temporal tau SUVr (r = 0.20, $P = 1.2 \times 10^{-4}$) [Fig. 4]. Aβ SUVr was inversely related to global cortical thickness (r = −0.14, $P = 3.0 \times 10^{-9}$), partially attenuated after adjusting for network atrophy and demographics (partial r = −0.09, $P = 1.9 \times 10^{-4}$). Age was positively associated with network

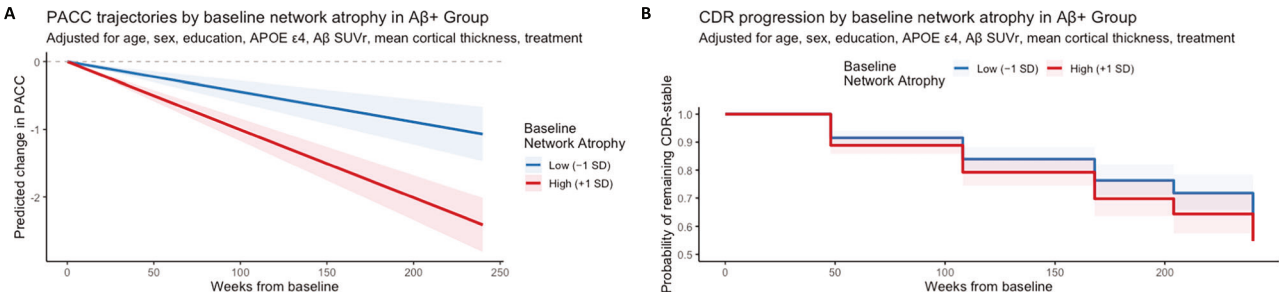

Fig. 5 Baseline Network Atrophy Predicts Longitudinal Cognitive and Functional Decline. A Model-predicted Preclinical Alzheimer's Cognitive Composite (PACC) change from baseline in the Aβ+(A4) subgroup, derived from a linear mixed-effects model with random intercepts and random slopes for time. Three trajectories are shown corresponding to low (−1 SD), mean, and high (+1 SD) baseline network atrophy, with all other covariates (age, sex, years of education, *APOE* ε4 carrier status, mean cortical thickness, Aβ PET SUVr, and treatment assignment) held at sample reference values. Shaded bands indicate 95% pointwise confidence intervals computed from the fixed-effects design matrix as a contrast from baseline; by construction, all three lines are anchored at zero at week 0. Greater baseline network atrophy was associated with steeper cognitive decline (Weeks × network atrophy: $\beta = -0.013$, SE = 0.003, $p < 0.001$; $n = 1150$ participants, 12,872 observations). **B** Covariate-adjusted survival curves from a Cox proportional-hazards model of global CDR progression in the Aβ+ subgroup, evaluated at low (−1 SD), mean, and high (+1 SD) baseline network atrophy with all other covariates held at sample reference values. Shaded bands indicate 95% pointwise confidence intervals; the y-axis is truncated at 0.5 to visualize the divergence between groups. Each 1-SD increase in baseline network atrophy was associated with a 15% higher hazard of CDR progression (HR = 1.15, 95% CI 1.05–1.27, $p = 0.004$; $n = 1057$ participants, 374 events). Follow-up was censored at week 240, the end of the placebo-controlled trial period. Detailed model coefficients are reported in Tables S2 (LME, Aβ+) and S7 (Cox, Aβ+). PACC preclinical Alzheimer's cognitive composite, CDR clinical dementia rating, LME linear mixed-effects, SD standard deviation, HR hazard ratio, CI confidence interval, SUVr standardized uptake value ratio, *APOE* ε4 apolipoprotein E ε4 allele.

atrophy ($r = 0.10$, $P = 3.0 \times 10^{-5}$) and inversely with global cortical thickness ($r = -0.30$, $P < 2.2 \times 10^{-16}$).

Additionally, network atrophy was associated with clinical features of AD. Lower PACC ($r = -0.08$, $P = 0.001$) and higher CFI total score ($r = 0.09$, $P < 0.001$), and with PACC subdomains and CFI as reported by both participants and study partners [Fig. 4]. Network atrophy was also associated with global anxiety (STAI-6 total: $r = 0.06$, $P < 0.05$) and worry ($r = 0.06$, $P < 0.01$), but not with depression, optimism (FTPS), lifetime death wishes, or lifetime suicide attempts [Fig. 4]. All cross-sectional associations remained significant after FDR correction [Table S1].

Atrophy network map for preclinical AD predicted longitudinal disease trajectory

Cognitive decline measured by PACC. In the Aβ+(A4) subgroup, baseline network atrophy significantly moderated the rate of PACC decline (Weeks × network atrophy: $\beta = -0.013$, SE = 0.003, $P < 0.001$; Table S2; $N = 1150$ / 12,872 observations). Greater baseline network atrophy was associated with steeper longitudinal decline, with predicted trajectories diverging across the ~5-year follow-up [Fig. 5A]. The interaction was not significant in the Aβ−(LEARN) subgroup ($\beta = -0.001$, $P = 0.43$; Table S3; $N = 529$ / 5523 observations), indicating that the cognitive-trajectory association is amyloid-dependent.

Semi-partial marginal R^2 (computed as the loss in marginal R^2 when each predictor's main effect and time interaction were removed; Supplementary Fig. 3A, Table S4) showed that in the Aβ + subgroup, network atrophy uniquely accounted for 0.86% of variance in PACC trajectories beyond age, sex, education, *APOE* ε4, mean cortical thickness, and Aβ PET SUVr — exceeding the unique contribution of *APOE* ε4 (0.77%) and below mean cortical thickness (2.89%) and Aβ PET SUVr (3.61%). In the Aβ− subgroup, the contribution was negligible (0.03%).

Sensitivity analyses adjusting for baseline tau attenuated the Weeks × network-atrophy interaction by 84% with inferior-temporal tau and 69% with the meta-temporal composite [Tables S5–S6], indicating that the cognitive-slope signal of network atrophy is largely shared with regional tau burden, despite only a modest bivariate correlation between the two measures ($r = 0.17$).

Functional decline measured by CDR-global progression. Among 1068 Aβ+ participants with CDR follow-up (380 progression events; 35.6%), each 1-SD increase in baseline network atrophy was associated with a 15% higher hazard of CDR progression (HR = 1.15, 95% CI 1.05–1.27, $P = 0.004$; Table S7). The full cohort showed a similar effect (HR = 1.14, 95% CI 1.05–1.25, $P = 0.003$; $N = 1568$, 462 events); the Aβ− subgroup showed a non-significant same-direction effect (HR = 1.09, 95% CI 0.89–1.34, $P = 0.40$; $N = 500$, 82 events; Table S8). Covariate-adjusted survival curves at low (−1 SD), mean, and high (+1 SD) baseline network atrophy showed divergent CDR-progression probabilities [Fig. 5B], and a forest plot of all covariate effects is provided [Supplementary Fig. 3B]. The proportional-hazards assumption was satisfied (cox.zph GLOBAL $P = 0.13$).

The network-atrophy effect on both PACC slope and CDR progression was virtually unchanged when Aβ SUVr and global cortical thickness were excluded from the covariate set (LME β: −0.0125 vs −0.0125; Cox HR: 1.155 vs 1.155), confirming that the prognostic value of network atrophy is independent of these established AD biomarkers.

In the tau subcohort ($N = 358$ in A4, 138 events), tau adjustment attenuated the network-atrophy HR by only 13.5% with inferior-temporal tau (1.170→1.146) and 8.1% with meta-temporal tau (1.170→1.155); the full-cohort meta-tau-adjusted estimate remained significant (HR = 1.167, $P = 0.046$; Tables S9–S10). The magnitude of the network-atrophy hazard was preserved in tau-adjusted models, although the formal *P*-value moved from 0.049 to 0.09 in the smaller A4 tau subsample — a sample-size-driven loss of statistical certainty.

DISCUSSION

This study identified a distinct network-level pattern of atrophy in cognitively unimpaired older adults from a large AD-prevention cohort [11, 12] — a "preclinical AD network" highly similar to the previously established AD-dementia atrophy network [10]. Atrophy connectivity to this network, 'network atrophy,' was independently associated with Aβ pathology, regional tau burden, lower cognition, greater subjective cognitive decline, and self-reported anxiety, and predicted both faster PACC decline and a higher hazard of CDR progression over ~5 years of follow-up. Effects were amyloid-dependent: present in Aβ+ but not Aβ− participants, indicating that the prognostic value of network atrophy reflects engagement of the AD pathological cascade rather than normal aging.

A key feature of this measure is that network atrophy provides prognostic information that is largely independent of conventional

cortical-thickness and Aβ-PET measures. Although individual vertex-wise cortical-thickness reductions form the input to network mapping, the resulting connectivity-based measure was uncorrelated with total atrophy (global cortical thickness; $r = 0.04$, $P = 0.12$), and the longitudinal-trajectory associations of network atrophy persisted after adjustment for total atrophy. Network atrophy was positively but modestly associated with Aβ ($r = 0.16$, $P < 0.001$), consistent with its interpretation as a marker of AD-related pathological burden; however, the LME and Cox effect sizes for network atrophy were virtually unchanged when both Aβ and total atrophy were removed from the covariate set (LME β: −0.0125 → −0.0125; Cox HR: 1.155→1.155). The semi-partial R^2 for network atrophy in PACC trajectories (0.86% in Aβ+) added uniquely to those of total atrophy (2.89%) and Aβ (3.61%). Together, these results indicate that what network atrophy captures is not total volume loss or global amyloid burden but the spatial topography of atrophy — its alignment with AD-vulnerable functional networks.

A notable dissociation also emerged when network atrophy and regional tau were considered jointly. For continuous cognitive slope (PACC), baseline tau accounted for ~80% of network atrophy's longitudinal effect, indicating that tau and the slope-relevant subset of network-atrophy variance are largely shared — even though the two measures correlate only modestly cross-sectionally (r≈0.17). In contrast, for clinical-milestone progression (CDR), baseline tau accounted for only ~10% of network atrophy's hazard, and the network-atrophy effect was preserved at near-original magnitude. This pattern indicates that network atrophy and regional tau capture predominantly *independent* prognostic information for clinical progression, even when they share most of the slope-relevant signal for continuous cognitive change. Mechanistically, this is consistent with network-level structural integrity reflecting accumulated downstream neurodegeneration [41] that is partially distinct from regional tau topography, and with clinical-milestone progression depending on factors — global brain reserve, network-level resilience [42], comorbid pathology [43] — not fully captured by regional tau burden alone.

The detection of network-specific atrophy in preclinical AD also has implications for the biological framing of the disease. Although AD neuropathology accrues years before symptoms [1], leading to a biological definition of preclinical AD [44], some have questioned whether this asymptomatic stage constitutes a distinct disease entity [45]. Our results demonstrate that AD-specific network-level neurodegeneration is detectable in preclinical AD, supporting the view that preclinical AD is not merely a risk factor but an early phase of the AD disease process.

ANM extends the atrophy-network framework established by Tetreault et al. [10] for AD dementia into the preclinical stage. ANM was more sensitive than direct vertex-wise atrophy comparisons in our cohort, which detected only scattered small clusters with continuous Aβ SUVr and no regions in dichotomous Aβ comparisons. Convergent results across Aβ-based and tau-based ANM, despite a smaller tau subsample, support the robustness of the network. The strongest tau-related effect was for inferior-temporal tau, consistent with prior findings of tight Aβ–tau coupling in this region in CU older adults [46].

The cross-sectional association of network atrophy with anxiety and worry — but not with depression, optimism, or suicidality measures — is consistent with our previous work suggesting that anxiety, particularly worry, may be a salient neuropsychiatric symptom of preclinical AD [47]. This specificity is biologically informative. Late-life neuropsychiatric symptoms have heterogeneous etiologies, and the demonstration that worry but not depression or suicidality co-localizes with AD-vulnerable network atrophy supports the position that worry in this population may reflect early AD-related neurodegeneration rather than nonspecific mood disturbance. The default-mode and frontoparietal regions in our preclinical AD network — particularly medial prefrontal cortex, precuneus, and lateral parietal cortex — substantially overlap with circuits implicated in repetitive negative thinking and self-referential processing in psychiatric populations [48], suggesting that early network-level structural disruption may manifest as elevated worry before objective cognitive impairment is apparent. These observations support a biological-psychiatric framing of preclinical AD in which neuropsychiatric symptoms are not nonspecific epiphenomena but topographically constrained manifestations of AD-related network neurodegeneration — directly relevant to the broader question of whether preclinical AD constitutes a distinct clinical-biological entity [45].

The preclinical AD network localized to the right dorsolateral and medial prefrontal cortex, bilateral precuneus, bilateral lateral parietal lobes, and right middle temporal gyrus — key default-mode-network regions affected in AD [49, 50]. The medial temporal lobe did not survive correction. This may reflect selection bias: subjects with medial temporal involvement are more likely to be symptomatic and excluded from preclinical-stage cohorts [51]. The asymmetry could reflect a similar bias, with left-hemisphere atrophy producing language-related deficits more likely to lead to symptomatic-stage exclusion [52, 53].

These findings raise the possibility that network atrophy mapping, derived from a single structural MRI, could provide clinically actionable information without requiring resource-intensive ancillary workups such as Aβ or tau PET imaging or fluid biomarkers. In our analyses, network atrophy was independently associated with both AD pathology and longitudinal cognitive and functional trajectories — measures typically available only through targeted radiotracer or assay-based testing. Although the absolute effect sizes were modest, structural MRI is widely available, relatively low-cost, requires no radioactive tracers or specialized blood assays, and could in principle support a first-pass triage to identify cognitively unimpaired individuals at increased AD-pathway risk for subsequent confirmatory testing. This clinical potential will require prospective validation in independent cohorts, derivation of clinically meaningful thresholds, and demonstration that network-atrophy-based prediction adds value over existing structural-MRI risk algorithms (e.g., AD-signature volumetry, hippocampal volume). Establishing these benchmarks is a necessary next step toward deploying atrophy network mapping as a non-invasive screening biomarker in preclinical AD.

This study has limitations. Effect sizes are modest because preclinical-stage participants have minimal atrophy and minimal symptoms, limiting explainable variance. We did not account for other neurodegenerative processes (e.g., Lewy bodies, TDP-43), although our cohort reflects a real-world preclinical-AD population per current diagnostic criteria [43, 54]. Follow-up was ~5 years; longer follow-up and serial tau-PET acquisitions would clarify whether network atrophy can serve as a stand-alone prognostic marker or is best deployed jointly with tau imaging. Tau analyses were limited by the smaller tau-PET subsample, contributing to sample-size–driven loss of statistical certainty in the A4 tau-adjusted Cox model. Future external validation in prospective longitudinal cohorts will be necessary before clinical deployment.

In summary, network-level neurodegeneration is detectable in preclinical AD using ANM and predicts both cognitive and functional decline, with effects that are amyloid-dependent, independent of total cortical atrophy, and partially independent of regional tau burden. These findings support preclinical AD as an early disease stage, validate ANM at this stage, and motivate future investigation of network atrophy as a non-invasive prognostic biomarker and potential therapeutic target.

DATA AVAILABILITY

The A4/LEARN data are publicly available online at the Image and Data Archive (https://ida.loni.usc.edu). All code used in the analysis and the maps generated in this study will be available upon request. Requests can be sent to the corresponding author (soyoung.lee@bwh.harvard.edu).

REFERENCES

1. Jack CR Jr., Knopman DS, Jagust WJ, Petersen RC, Weiner MW, Aisen PS, et al. Tracking pathophysiological processes in Alzheimer's disease: an updated hypothetical model of dynamic biomarkers. Lancet Neurol. 2013;12:207–16.
2. Dubois B, Hampel H, Feldman HH, Scheltens P, Aisen P, Andrieu S, et al. Preclinical Alzheimer's disease: definition, natural history, and diagnostic criteria. Alzheimer's Dement. 2016;12:292–323.
3. Dickerson BC, Bakkour A, Salat DH, Feczko E, Pacheco J, Greve DN, et al. The cortical signature of Alzheimer's disease: regionally specific cortical thinning relates to symptom severity in very mild to mild AD dementia and is detectable in asymptomatic amyloid-positive individuals. Cereb Cortex. 2009;19:497–510.
4. Becker JA, Hedden T, Carmasin J, Maye J, Rentz DM, Putcha D, et al. Amyloid-β associated cortical thinning in clinically normal elderly. Ann Neurol. 2011;69:1032–42.
5. Josephs KA, Whitwell JL, Ahmed Z, Shiung MM, Weigand SD, Knopman DS, et al. Beta-amyloid burden is not associated with rates of brain atrophy. Ann Neurol. 2008;63:204–12.
6. Chételat G, Villemagne VL, Pike KE, Baron JC, Bourgeat P, Jones G, et al. Larger temporal volume in elderly with high versus low beta-amyloid deposition. Brain. 2010;133:3349–58.
7. Pegueroles J, Vilaplana E, Montal V, Sampedro F, Alcolea D, Carmona-Iragui M, et al. Longitudinal brain structural changes in preclinical Alzheimer's disease. Alzheimer's Dement. 2017;13:499–509.
8. Xie L, Wisse LEM, Das SR, Vergnet N, Dong M, Ittyerah R, et al. Longitudinal atrophy in early braak regions in preclinical Alzheimer's disease. Hum Brain Mapp. 2020;41:4704–17.
9. Fox MD. Mapping symptoms to brain networks with the human connectome. N Engl J Med. 2018;379:2237–45.
10. Tetreault AM, Phan T, Orlando D, Lyu I, Kang H, Landman B, et al. Network localization of clinical, cognitive, and neuropsychiatric symptoms in Alzheimer's disease. Brain. 2020;143:1249–60.
11. Sperling RA, Donohue MC, Raman R, Rafii MS, Johnson K, Masters CL, et al. Trial of solanezumab in preclinical Alzheimer's disease. N Engl J Med. 2023;389:1096–107.
12. Sperling RA, Donohue MC, Raman R, Sun C-K, Yaari R, Holdridge K, et al. Association of factors with elevated amyloid burden in clinically normal older individuals. JAMA Neurol. 2020;77:735–45.
13. Petersen RC, Aisen PS, Beckett LA, Donohue MC, Gamst AC, Harvey DJ, et al. Alzheimer's disease neuroimaging initiative (ADNI): clinical characterization. Neurology. 2010;74:201–9.
14. Mormino EC, Papp KV, Rentz DM, Donohue MC, Amariglio R, Quiroz YT, et al. Early and late change on the preclinical Alzheimer's cognitive composite in clinically normal older individuals with elevated amyloid β. Alzheimers Dement. 2017;13:1004–12.
15. Donohue MC, Sperling RA, Salmon DP, Rentz DM, Raman R, Thomas RG, et al. The preclinical alzheimer cognitive composite: measuring amyloid-related decline. JAMA Neurol. 2014;71:961–70.
16. Amariglio RE, Donohue MC, Marshall GA, Rentz DM, Salmon DP, Ferris SH, et al. Tracking early decline in cognitive function in older individuals at risk for Alzheimer disease dementia: the Alzheimer's disease cooperative study cognitive function instrument. JAMA Neurol. 2015;72:446–54.
17. Amariglio RE, Sikkes SAM, Marshall GA, Buckley RF, Gatchel JR, Johnson KA, et al. Item-level investigation of participant and study partner report on the cognitive function index from the A4 study screening data. J Prev Alzheimers Dis. 2021;8:257–62.
18. Morris JC. The clinical dementia rating (CDR): current version and scoring rules. Neurology. 1993;43:2412–4.
19. Marteau TM, Bekker H. The development of a six-item short-form of the state scale of the Spielberger state—trait anxiety inventory (STAI). Br J Clin Psychol. 1992;31:301–6.
20. Yesavage JA, Sheikh JI. 9/Geriatric depression scale (GDS). Clin Gerontol. 1986;5:165–73.
21. Zimbardo PG, Boyd JN. Putting time in perspective: a valid, reliable individual-differences metric. J Pers Soc Psychol. 1999;77:1271–88.
22. Fischl B. FreeSurfer. Neuroimage. 2012;62:774–81.
23. Heister D, Brewer JB, Magda S, Blennow K, McEvoy LK. Predicting MCI outcome with clinically available MRI and CSF biomarkers. Neurology. 2011;77:1619–28.
24. Johnson KA, Sperling RA, Gidicsin CM, Carmasin JS, Maye JE, Coleman RE, et al. Florbetapir (F18-AV-45) PET to assess amyloid burden in Alzheimer's disease dementia, mild cognitive impairment, and normal aging. Alzheimers Dement. 2013;9:S72–83.
25. Young CB, Winer JR, Younes K, Cody KA, Betthauser TJ, Johnson SC, et al. Divergent cortical tau positron emission tomography patterns among patients with preclinical alzheimer disease. JAMA Neurol. 2022;79:592–603.
26. Greve DN, Svarer C, Fisher PM, Feng L, Hansen AE, Baare W, et al. Cortical surface-based analysis reduces bias and variance in kinetic modeling of brain PET data. Neuroimage. 2014;92:225–36.
27. Greve DN, Salat DH, Bowen SL, Izquierdo-Garcia D, Schultz AP, Catana C, et al. Different partial volume correction methods lead to different conclusions: an (18) F-FDG-PET study of aging. Neuroimage. 2016;132:334–43.
28. The MathWorks I. MATLAB version: 9.13.0 (R2022b). 2022.
29. Team RC. R: A Lang Environ Stat computing Vienna, Austria: R Foundation for Statistical Computing; 2023. <https://www.R-project.org>
30. Altman DG, Royston P. The cost of dichotomising continuous variables. BMJ. 2006;332:1080.
31. Westfall PH, Young SS Resampling-based multiple testing: examples and methods for p-value adjustment. John Wiley & Sons; 1993. 279.
32. Yeo BTT, Krienen FM, Sepulcre J, Sabuncu MR, Lashkari D, Hollinshead M, et al. The organization of the human cerebral cortex estimated by intrinsic functional connectivity. J Neurophysiol. 2011;106:1125–65.
33. Holmes AJ, Hollinshead MO, O'Keefe TM, Petrov VI, Fariello GR, Wald LL, et al. Brain genomics superstruct project initial data release with structural, functional, and behavioral measures. Sci Data. 2015;2:150031.
34. Winkler AM, Ridgway GR, Webster MA, Smith SM, Nichols TE. Permutation inference for the general linear model. Neuroimage. 2014;92:381–97.
35. Braak H, Alafuzoff I, Arzberger T, Kretzschmar H, Del Tredici K. Staging of alzheimer disease-associated neurofibrillary pathology using paraffin sections and immunocytochemistry. Acta Neuropathol. 2006;112:389–404.
36. Braak H, Braak E. Neuropathological stageing of Alzheimer-related changes. Acta Neuropathol. 1991;82:239–59.
37. Jack CR Jr., Wiste HJ, Weigand SD, Therneau TM, Lowe VJ, Knopman DS, et al. Defining imaging biomarker cut points for brain aging and Alzheimer's disease. Alzheimer's Dement. 2017;13:205–16.
38. Nadeau C, Bengio Y. Inference for the Generalization Error. Machine Learning 2003;52:239–281.
39. Benjamini Y, Hochberg Y. Controlling the False Discovery Rate: A Practical and Powerful Approach to Multiple Testing. Journal of the Royal Statistical Society: Series B (Methodological) 1995;57:289–300.
40. Stoffel MA, Nakagawa S, Schielzeth H. partR2: partitioning R(2) in generalized linear mixed models. PeerJ. 2021;9:e11414.
41. Seeley WW, Crawford RK, Zhou J, Miller BL, Greicius MD. Neurodegenerative diseases target large-scale human brain networks. Neuron. 2009;62:42–52.
42. Stern Y, Arenaza-Urquijo EM, Bartrés-Faz D, Belleville S, Cantilon M, Chetelat G, et al. Whitepaper: defining and investigating cognitive reserve, brain reserve, and brain maintenance. Alzheimers Dement. 2020;16:1305–11.
43. Robinson JL, Lee EB, Xie SX, Rennert L, Suh E, Bredenberg C, et al. Neurodegenerative disease concomitant proteinopathies are prevalent, age-related and APOE4-associated. Brain. 2018;141:2181–93.
44. Jack CR Jr., Bennett DA, Blennow K, Carrillo MC, Dunn B, Haeberlein SB, et al. NIA-AA research framework: toward a biological definition of Alzheimer's disease. Alzheimers Dement. 2018;14:535–62.
45. Dubois B, Villain N, Schneider L, Fox N, Campbell N, Galasko D, et al. Alzheimer disease as a clinical-biological construct—an international working group recommendation. JAMA Neurol. 2024;81:1304–11.
46. Insel PS, Young CB, Aisen PS, Johnson KA, Sperling RA, Mormino EC, et al. Tau positron emission tomography in preclinical Alzheimer's disease. Brain. 2023;146:700–11.
47. Lee S, Zide BS, Palm ST, Drew WJ, Sperling RA, Jacobs HIL, et al. Specific association of worry with amyloid-β but not tau in cognitively unimpaired older adults. Am J Geriatr Psychiatry. 2024;32:1203–14.
48. Hamilton JP, Farmer M, Fogelman P, Gotlib IH. Depressive rumination, the default-mode network, and the dark matter of clinical neuroscience. Biol Psychiatry. 2015;78:224–30.
49. Sperling RA, Laviolette PS, O'Keefe K, O'Brien J, Rentz DM, Pihlajamaki M, et al. Amyloid deposition is associated with impaired default network function in older persons without dementia. Neuron. 2009;63:178–88.
50. Greicius MD, Srivastava G, Reiss AL, Menon V. Default-mode network activity distinguishes Alzheimer's disease from healthy aging: evidence from functional MRI. Proc Natl Acad Sci USA. 2004;101:4637–42.
51. Dickerson BC, Stoub TR, Shah RC, Sperling RA, Killiany RJ, Albert MS, et al. Alzheimer-signature MRI biomarker predicts AD dementia in cognitively normal adults. Neurology. 2011;76:1395–402.
52. Gorno-Tempini ML, Hillis AE, Weintraub S, Kertesz A, Mendez M, Cappa SF, et al. Classification of primary progressive aphasia and its variants. Neurology. 2011;76:1006–14.
53. Migliaccio R, Agosta F, Possin KL, Canu E, Filippi M, Rabinovici GD, et al. Mapping the progression of atrophy in early- and late-onset Alzheimer's disease. J Alzheimers Dis. 2015;46:351–64.

54. Jack CR Jr., Andrews JS, Beach TG, Buracchio T, Dunn B, Graf A, et al. Revised criteria for diagnosis and staging of Alzheimer's disease: Alzheimer's association workgroup. Alzheimer's Dement. 2024;20:5143–69.

ACKNOWLEDGEMENTS

The A4 Study is a secondary prevention trial in preclinical Alzheimer's disease, aiming to slow cognitive decline associated with brain amyloid accumulation in clinically normal older individuals. The A4 Study is funded by a public-private-philanthropic partnership, including funding from the National Institutes of Health-National Institute on Aging, Eli Lilly and Company, Alzheimer's Association, Accelerating Medicines Partnership, GHR Foundation, an anonymous foundation and additional private donors, with in-kind support from Avid and Cogstate. The companion observational Longitudinal Evaluation of Amyloid Risk and Neurodegeneration (LEARN) Study is funded by the Alzheimer's Association and GHR Foundation. The A4 and LEARN Studies are led by Dr. Reisa Sperling at Brigham and Women's Hospital, Harvard Medical School and Dr. Paul Aisen at the Alzheimer's Therapeutic Research Institute (ATRI), University of Southern California. The A4 and LEARN Studies are coordinated by ATRI at the University of Southern California, and the data are made available through the Laboratory for Neuro Imaging at the University of Southern California. The participants screening for the A4 Study provided permission to share their de-identified data in order to advance the quest to find a successful treatment for Alzheimer's disease. We would like to acknowledge the dedication of all the participants, the site personnel, and all of the partnership team members who continue to make the A4 and LEARN Studies possible. The complete A4 Study Team list is available at: a4study.org/a4-study-team. Data collection and sharing for the Alzheimer's Disease Neuroimaging Initiative (ADNI) is funded by the National Institute on Aging (National Institutes of Health Grant U19 AG024904). The grantee organization is the Northern California Institute for Research and Education. In the past, ADNI has also received funding from the National Institute of Biomedical Imaging and Bioengineering, the Canadian Institutes of Health Research, and private sector contributions through the Foundation for the National Institutes of Health (FNIH) including generous contributions from the following: AbbVie, Alzheimer's Association; Alzheimer's Drug Discovery Foundation; Araclon Biotech; BioClinica, Inc.; Biogen; Bristol-Myers Squibb Company; CereSpir, Inc.; Cogstate; Eisai Inc.; Elan Pharmaceuticals, Inc.; Eli Lilly and Company; EuroImmun; F. Hoffmann-La Roche Ltd and its affiliated company Genentech, Inc.; Fujirebio; GE Healthcare; IXICO Ltd.; Janssen Alzheimer Immunotherapy Research & Development, LLC.; Johnson & Johnson Pharmaceutical Research &Development LLC.; Lumosity; Lundbeck; Merck & Co., Inc.; Meso Scale Diagnostics, LLC.; NeuroRx Research; Neurotrack Technologies; Novartis Pharmaceuticals Corporation; Pfizer Inc.; Piramal Imaging; Servier; Takeda Pharmaceutical Company; and Transition Therapeutics.

AUTHOR CONTRIBUTIONS

S Lee and SHS conceived and designed the study. S Lee, SRB, JHH, STP, WJD, GTB, and BSZ processed the data. S Lee, SRB, GTB, STP, WJD, BSZ, NMC, S Lariviere, SZ, and BTTY developed the methodology and conducted the investigation. S Lee, SZ, and SHS performed the neuroimaging and statistical analyses and created the visualizations. S Lee wrote the original draft. MDF, RAS, NJD, BTTY, and SHS provided high-level supervision and project guidance. All authors contributed to data interpretation, reviewed and edited the manuscript, and approved the final version of the manuscript.

FUNDING

Stuart T. Hauser Research Training Program in Biological and Social Psychiatry at Judge Baker Children's Center, National Institute of Mental Health, National Institutes of Health, under Grant Number 2T32MH016259-34, philanthropic gifts (the Neuropsychiatry of Aging Research Fund and the Geriatric Psychiatry Fund) to the Division of Geriatric Psychiatry, Department of Psychiatry and the Center for Brain Circuit Therapeutics, Brigham and Women's Hospital (SLee). National Institute of Mental Health grant K23MH121657, National Institute of Mental Health grant R21MH126271, Brain and Behavior Research Foundation Young Investigator Grant, Baszucki Brain Research Fund and the Department of Veterans Affairs grant I01CX002293 (SHS). BTTY is supposed by the NUS Yong Loo Lin School of Medicine (NUHSRO/2020/124/TMR/LOA), the Singapore National Medical Research Council (NMRC) LCG (OFLCG19May-0035), NMRC CTG-IIT (CTGIIT23jan-0001), NMRC OF-IRG (OFIRG24jan-0006; OFIRG24jul-0049), NMRC STaR (STaR20nov-0003), Singapore Ministry of Health (MOH) Centre Grant (CG21APR1009), the United States National Institutes of Health (R01MH133334 & 2R01MH120080) and the Singapore National Research Foundation (NRF) Investigatorship (NRFI10-2024-0014). Any opinions, findings and conclusions or recommendations expressed in this material are those of the authors and do not reflect the views of the funders.

COMPETING INTERESTS

There are no personal financial conflicts of interest related to the present results. SLee, SRB, GTB, STP, WJD, BSZ, NMC, and SLariviere report no conflicts with any concept discussed in this article. MDF reports consulting fees from Magnus Medical, Sorterix, Abott, and Boston Scientific. MDF also owns independent intellectual property involving the use of functional connectivity to target TMS for depression, which was filed in 2013, has yielded no royalties and does not cover the present work. RAS has served as a paid consultant for AbbVie, AC Immune, Acumen, Alector, Apellis, Biohaven, Bristol Myers Squibb, Genentech, Ionis, Janssen, Oligomerix, Prothena, Roche, and Vaxxinity. She has received research funding from Eisai and Eli Lilly for public-private partnership clinical trials and receives research grant funding from the National Institute on Aging/National Institutes of Health, GHR Foundation, and the Alzheimer's Association. Her spouse, K. Johnson, reports consulting fees from Novartis, Merck, and Janssen. NJD reports receiving royalties from the American Psychiatric Association Press, and honoraria and travel support for Harvard University, Harvard Medical School, and NIH-sponsored events. SHS is an owner of intellectual property involving the use of individualized resting-state network mapping to target TMS, which was filed in 2016, has yielded no royalties and does not cover the present work. SHS is also a scientific consultant for Magnus Medical, received investigator-initiated research funding from Neuronetics (2019) and Brainsway (2022), received speaking fees from Brainsway (2021) and Otsuka (for PsychU.org, 2021), and is a shareholder in Brainsway (publicly traded) and Magnus Medical (not publicly traded).

ETHICAL APPROVAL

The A4 (ClinicalTrials.gov: NCT02008357) and LEARN (ClinicalTrials.gov: NCT02488720) studies were coordinated by the Alzheimer's Therapeutic Research Institute (ATRI) at the University of Southern California. Ethical approval was obtained from the institutional review board at each of the 67 participating sites in the United States, Canada, Japan, and Australia. All participants and their study partners provided written informed consent prior to data collection, including consent for data sharing. All methods were performed in accordance with the ethical standards of the responsible institutional review boards and with the Helsinki Declaration of 1975 (as revised in 1983).

ADDITIONAL INFORMATION

Supplementary information The online version contains supplementary material available at https://doi.org/10.1038/s41380-026-03706-0.

Correspondence and requests for materials should be addressed to Soyoung Lee.

Reprints and permission information is available at http://www.nature.com/reprints

Publisher's note Springer Nature remains neutral with regard to jurisdictional claims in published maps and institutional affiliations.